Acta Materialia 124 (2017) 372–382

Contents lists available at ScienceDirect

Acta Materialia

journal homepage: www.elsevier.com/locate/actamat

Full length article

<c+a> dislocations and their interactions with other crystal defects in a Mg alloy

W.W. Hu [a, b], Z.Q. Yang [a, *], H.Q. Ye [a]

[a] Shenyang National Laboratory for Materials Science, Institute of Metal Research, Chinese Academy of Science, Shenyang 110016, China
[b] University of Chinese Academy of Sciences, Beijing 100039, China

ARTICLE INFO

Article history:
Received 7 September 2016
Received in revised form
4 November 2016
Accepted 6 November 2016
Available online 16 November 2016

Keywords:
Mg alloy
<**c**+**a**> dislocation
Plastic deformation
Ductility
Grain boundary

ABSTRACT

<**c**+**a**> dislocations and their interactions with other crystal defects in a Mg alloy have been investigated using atomic-resolution aberration-corrected scanning transmission electron microscopy. Two types of <**c**+**a**> dislocations, with either a 60° or a screw <**a**> component, were observed in Mg matrix, and both of them could form low-angle tilt grain boundaries during plastic deformation. <**c**+**a**> dislocations could lead to migration of grain boundaries formed previously by <**a**> dislocations in deformed Mg matrix. Moving <**c**+**a**> dislocations cut and reacted with basal stacking faults, producing new defect structures during deformation. The mechanisms for interaction/reaction between <**c**+**a**> dislocations and other defects are modeled based on atomic-resolution observations. These experimental results provide clear evidence for the occurrence of long range motion of <**c**+**a**> dislocations with relatively compact cores during plastic deformation, instead of immediate dissociation on basal planes.

1. Introduction

Mg alloys have tremendous potential to achieve energy efficiency in many industries including aerospace and automotive, since they are the lightest metallic materials for structural applications [1,2]. But hexagonal close-packed (HCP) Mg alloys usually exhibit ductility not high enough for making structural components through plastic processing. The poor formability of Mg alloys is due to the fact that their easiest slip system, $(0001) < 11\bar{2}0 >$, cannot supply five independent slip systems to satisfy the von Mises criterion for homogeneous plastic deformation in polycrystalline materials [3,4]. Improvement of ductility is thus very important for the applications of Mg alloys. Additionally, basal slip cannot accommodate deformation along c-axis, which might result in high anisotropy in the plastic deformation, consequently impairing the formability of Mg alloys. Both <**c**+**a**> slip and deformation twinning can produce deformation along c-axis in HCP materials [5,6]. Moreover, there are five independent pyramidal slip systems for <**c**+**a**> dislocations, so they may have strong influences on the ductility and strength of HCP alloys [5,7–9].

Mg alloys containing long period stacking ordered (LPSO) phases showed suitable ductility and excellent strength at both ambient and elevated temperatures [10–13]. But, deformation of the strengthening LPSO phases was known mediated by generation and motion of basal dislocations [13]. Moreover, deformation twinning was remarkably limited due to the large amount of stacking faults (SFs) or LPSO lamellae in LPSO-strengthened Mg alloys [13–15]. Therefore, there should be deformation modes other than twinning and basal slip, being activated, so that LPSO-strengthened Mg alloys can exhibit good strength and ductility. Motion of <**c**+**a**> dislocations might be a candidate for realization of homogeneous plastic deformation in these alloys [16–24]. However, previous molecular dynamics simulations showed that the poor ductility of Mg alloys was probably associated with <**c**+**a**> dislocations, since <**c**+**a**> dislocations could transform from dissociated geometry on pyramidal planes into sessile locks on basal planes in Mg [25,26]. It thus seems incapable to improve ductility of Mg alloys through activation of <**c**+**a**> dislocations. Interestingly, two-beam transmission electron microscopy observations found that <**c**+**a**> dislocations had relatively compact cores in Mg-Ce and Mg-Y alloys, implying that proper alloying might be able to modify the behavior of <**c**+**a**> dislocations, and hence improve the ductility of Mg alloys [18,20,27,28]. Therefore, further investigations on dislocations with atomic resolution, especially the <**c**+**a**> dislocations, are necessary, in order to understand their behavior on the atomic level during plastic deformation, and their

* Corresponding author.
E-mail address: yangzq@imr.ac.cn (Z.Q. Yang).

http://dx.doi.org/10.1016/j.actamat.2016.11.015
1359-6454/

contribution in Mg alloys with little capability of deformation twinning [13–15].

In the present work, we studied <**c**+**a**> dislocations in a LPSO-strengthened Mg-Zn-Y alloy using high-angle annular dark-field scanning-transmission electron microscopy (HAADF-STEM) (also known as Z-contrast) imaging with atomic resolution [29,30]. Besides dissociation of isolated <**c**+**a**> dislocations on basal planes and Suzuki segregation in deformed Mg grains [24], a variety of other defect structures and reactions, including low-angle grain boundaries (GBs) formed by rearrangement of <**c**+**a**> dislocations, GB migration induced by <**c**+**a**> dislocations, and reactions between <**c**+**a**> dislocations and basal SFs, were observed in plastically deformed samples. These defect structures and reactions associated with the generation and motion of <**c**+**a**> dislocations in Mg matrix should have important contribution to the ductility and strength of Mg alloys.

2. Experiments

A $Mg_{97}Zn_1Y_2$ (at.%) alloy was prepared using a high frequency melting furnace under protection of Ar atmosphere. Samples of size 10 mm in diameter and 20 mm in height were compressed by ~40% at a strain rate of 5×10^{-4} s^{-1} at 573 K. Specimens for microstructural investigations were cut in the direction parallel to the compression axis and prepared using standard ion milling techniques. Z-contrast observations were performed on an aberration-corrected Titan 60–300 microscope operating at 300 kV. The beam convergence half-angle was set as 25 mrad, and the collection half-angles of the HAADF detector ranged from about 60 mrad to about 290 mrad during atomic-resolution observations, which can effectively eliminate the influence of strain contrast around dislocations [29,30].

3. Results

Fig. 1a shows a schematic diagram of HCP structure for the description of characters and dissociation of dislocations in Mg with a stacking sequence of "$\cdots$ABAB$\cdots$". Vector ***AC*** indicates the view direction of $1/3<11\overline{2}0>$ for atomic-resolution observations of dislocations in the present work. 60° <**a**> dislocations with vector ***AB*** or ***BC*** and screw <**a**> dislocations with vector ***AC*** are denoted as <$\mathbf{a_{60}}$> and <$\mathbf{a_s}$>, respectively; **v**ectors $\boldsymbol{AA_0}$, $\boldsymbol{BB_0}$ and $\boldsymbol{CC_0}$ represent perfect <**c**> dislocations; vectors $\boldsymbol{AB_0}$ and $\boldsymbol{AC_0}$ are for <$\mathbf{c}+\mathbf{a_{60}}$> and <$\mathbf{c}+\mathbf{a_s}$> dislocations, respectively; vectors α ***A***, $\alpha\alpha_0$ and $\boldsymbol{A\alpha_0}$ represent the partial dislocations with Burgers vectors of $1/3<10\overline{1}0>$, $1/2<0001>$ and $1/6<20\overline{2}3>$, respectively. The stacking sequence of basal planes would change from "$\cdots$ABAB$\cdots$" to "$\cdots$ACAC$\cdots$" or "$\cdots$BCBC$\cdots$", if there was a basal stacking fault (SF) in the HCP structure. So, a schematic diagram for dislocations in an "$\cdots$ACAC$\cdots$"-stacked HCP structure is shown in Fig. 1b, in order to analyze dislocation-SF interactions. The pyramidal $\{10\overline{1}1\}$ plane is highlighted by green and red in Fig. 1a and b, respectively.

3.1. Basal slip

Fig. 2a shows a low-magnification Z-contrast image for microstructures in as-cast samples. Bright and dark regions represent the LPSO phase and α-Mg grain, respectively. The long straight bright lines in the α-Mg grain are very thin LPSO plates or growth SFs with Zn and Y segregation on basal planes [24]. Plates of LPSO phases are straight in the as-cast sample. Fig. 2b shows a low-magnification Z-contrast image recorded from a region containing many LPSO plates in the deformed sample, demonstrating formation of kink boundaries (KBs). These KBs were produced by rearrangement of 60° <**a**> dislocations during plastic deformation, and there are Cottrell atmospheres along the dislocations [31]. Fig. 3a shows an atomic-resolution Z-contrast image recorded from a region in Mg matrix next to a KB in deformed LPSO, demonstrating the formation of a low-angle (8°) GB with the same misorientation angle of the KB in the neighboring LPSO plate. Closure failure of Burgers circuits indicates that there is an array of basal <$\mathbf{a_{60}}$> dislocations. Fast Fourier transform (FFT) analysis (Fig. 3b) of the high resolution STEM image shows that the basal dislocations distribute homogeneously at the GB. The mean distance between neighboring dislocations is about 2 nm, from which a tilt angle of about 8° is calculated, which is consistent with the misorientation angle measured directly from the image shown in Fig. 3a.

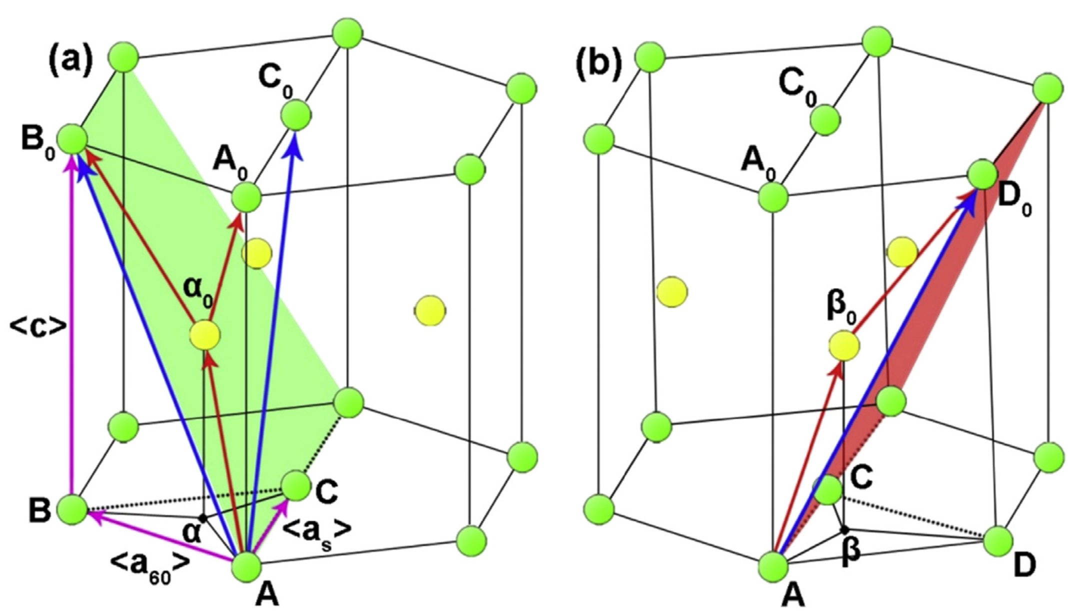

Fig. 1. Schematic diagram of Burgers vectors in Mg lattice, (a) "$\cdots$ABAB$\cdots$" stacking, (b) "$\cdots$ACAC$\cdots$" stacking.